

# Theoretical Analysis of Adsorption Properties and Vibrational Behavior of O<sub>2</sub> on Ag (110) Surface with Ab Initio CM and DAM Calculations

Kangnian Fan,\* Wenning Wang, and Jingfa Deng

Department of Chemistry, Fudan University, Shanghai 200433, P. R. China

(Received March 22, 1995)

Chemisorption properties and vibrational behaviors of molecular oxygen on Ag (110) surface have been studied by the cluster model (CM) and dipped adcluster model (DAM) with an Ag<sub>6</sub> cluster. Two stable states, <sup>1</sup>A<sub>1</sub> [ $\bar{1}\bar{1}0$ ] and <sup>3</sup>A<sub>2</sub> [001], have been found and assigned to peroxide (O<sub>2</sub><sup>2-</sup>) and superoxide (O<sub>2</sub><sup>-</sup>) species, respectively. Theoretically predicted adsorption geometries and vibrational frequencies for these states are similar to those measured in the experiments. With the DAM method, the calculated adsorption energies agree well with the experimental value. The O<sub>2</sub><sup>2-</sup> species is predicted to be more stable than the O<sub>2</sub><sup>-</sup> species. Cluster size and basis set effects have also been investigated.

Chemisorption of oxygen on a silver surface has been extensively studied both in experiments and theoretical calculations due to the specific activity of silver catalyst in partial oxidation processes.<sup>1)</sup> In particular, the single crystal Ag (110) was reported to be a better catalyst than the industrial form.<sup>2)</sup> Efforts to characterize the Ag (110)-O<sub>2</sub> system have resulted in a rough sketch of the O<sub>2</sub> adsorption, in which molecular oxygen exists as a precursor state for the dissociative adsorption.<sup>3,4)</sup>

Molecular adsorption oxygen has been identified on Ag (110) surfaces with an O-O stretching frequency at 640 cm<sup>-1</sup><sup>3)</sup> or 628 cm<sup>-1</sup>.<sup>4)</sup> Backx and co-workers<sup>4)</sup> proposed that the O<sub>2</sub> molecule adsorbs at a long bridge site with the bond axis parallel to the surface along the [ $\bar{1}\bar{1}0$ ] direction. UPS<sup>5,6)</sup> and NEXAFS<sup>7)</sup> results support the parallel adsorption model, but the ESDIAD<sup>8)</sup> experiment gave evidence that the bond axis is along [001] azimuth and tilts on the surface.

In theoretical treatments, the long bridge site model has been adopted. Selmani et al.<sup>9)</sup> reported LCGTO-LSD calculations of Ag<sub>4</sub>-O<sub>2</sub> with the optimum geometry of O-O bond axis parallel to the surface and oriented at 30° with respect to [001] direction. They also found the geometry with the O-O bond perpendicular to the surface has almost the same energy as the most stable one. Upton et al.<sup>10)</sup> performed GVB-CI calculations on Ag<sub>24</sub>-O<sub>2</sub>, in which an 11-electron ECP was used for the four silver atoms nearest the oxygen and a one-electron ECP for the others. They found the O<sub>2</sub> parallel adsorption at [ $\bar{1}\bar{1}0$ ] direction to be the most stable geometry, but the adsorption energies are all negative. Consequently, they argued that O<sub>2</sub> bonds to the low excited states of Ag<sub>24</sub>.

Most of the theoretical studies have been based on

the conventional cluster model, which neglects the effect of bulk metal. Nakatsuji<sup>11)</sup> has proposed a model named dipped adcluster model (DAM), in which a combined system, called an adcluster, of an admolecule and a metal cluster is dipped into the electron bath of the solid metal and an equilibrium is established for electron exchange between the adcluster and the bulk metal. The exchange is controlled by a balance of the chemical potentials of the adcluster and metal surface. With this model, Nakatsuji and Nakai<sup>12,13)</sup> investigated O<sub>2</sub> chemisorption and dissociation processes by the use of Ag<sub>2</sub>O<sub>2</sub> and Ag<sub>4</sub>O<sub>2</sub> adclusters. Positive chemisorption energies close to the experimental results<sup>14)</sup> were obtained in a Ag<sub>2</sub>O<sub>2</sub> system with one electron transferred from bulk metal. Two different molecular adsorption states have been predicted, namely peroxide (O<sub>2</sub><sup>2-</sup>) and superoxide (O<sub>2</sub><sup>-</sup>) species, and the O<sub>2</sub><sup>-</sup> is the low excited state. As an illustration for the Ag (110) surface, however, the adsorption site with the O-O bond along [001] direction has not been considered.

Molecular adsorbed superoxide (O<sub>2</sub><sup>-</sup>) species has been detected on single crystal Ag (111) surface,<sup>15)</sup> polycrystalline,<sup>16,17)</sup> and electrolytic silver,<sup>18)</sup> although it has never been reported on Ag (110) surface. Our very recent in situ Raman study<sup>18)</sup> on electrolytic silver has shown that both O<sub>2</sub><sup>2-</sup> and O<sub>2</sub><sup>-</sup> species exist on a silver surface over a large region of temperature from 298 to 673 K. It seems more likely that the O<sub>2</sub><sup>-</sup> species is a ground state with different adsorption geometry rather than an excited state relative to the peroxide (O<sub>2</sub><sup>2-</sup>) species. Theoretical studies by Broomfield et al.<sup>19)</sup> and Nakatsuji et al.<sup>20)</sup> showed the existence of the end-on adsorption in a Ag-O<sub>2</sub> system, with the O-O axis being bent about 70 degrees from the surface nor-

mal, while the superoxide (O<sub>2</sub><sup>-</sup>) species is the ground state in this geometry. In this paper, a 6-atom Ag cluster has been used to model the C<sub>2v</sub> symmetric long bridge adsorption site on Ag (110) surface, and three adsorbate geometries retaining C<sub>2v</sub> symmetry have been considered, viz., geometries with the O–O bond parallel to the surface along either [110] or [001] directions and with the O–O bond perpendicular to the surface pointing to the center of the long bridge site. Their adsorption properties and vibrational behaviors have been investigated. It is worth mentioning that the geometry with O–O bond axis tilting on the surface at long bridge site which breaks the C<sub>2v</sub> symmetry has higher energy than the parallel geometry. Therefore no stable end-on adsorption shown by Broomfield et al.<sup>19)</sup> and Nakatsuji et al.<sup>20)</sup> has been found in our work, the reason for which may be due to the fact that there are two Ag atoms interacting directly with an O<sub>2</sub> molecule at the long bridge site. The situation is quite different in the Ag–O<sub>2</sub> system, in which only one atom is included in the adsorption system adopted by the above authors. In consideration of the symmetric aspect, the parallel geometry is reasonably preferred at a long bridge site. Among the three adsorption geometries with C<sub>2v</sub> symmetry, the perpendicular one was found to have much higher energy than the other two parallel ones and has been ruled out. Both the cluster and dipped adcluster models were employed to investigate the influence of bulk metal on the chemisorption energy of a limited cluster. The effects of cluster size and basis set are also discussed.

### Computational Details

An 11-electron relativistic effective core potential<sup>21)</sup> was used for all Ag atoms, with two kinds of Gaussian basis sets, (3s3p4d/2s2p2d) (Set I) and (3s3p4d/2s1p1d) (Set II). For oxygen, we used the (9s5p/3s2p) Gaussian set of Huzinaga–Dunning augmented with a single set of polarization *d* functions ( $\zeta=0.85$ ).<sup>22)</sup> All calculations were performed at the HF level (RHF for singlet states and ROHF for doublet and triplet ones) by the use of the programs GAMESS<sup>23)</sup> and Gaussian 92 for Windows.<sup>24)</sup> The Ag–Ag bond distance was fixed at 2.89 Å during the optimization of both the O–O bond length and Ag–O perpendicular distance. For DAM, the total energy of the system was

calculated by using HF procedure with the electrostatic image force correction,<sup>25)</sup> which is characteristic of a metal surface.<sup>26)</sup>

### Results and Discussion

We choose an Ag<sub>6</sub> cluster (Fig. 1) with two atoms in each layer to model the long bridge site of the Ag (110) surface. The calculated results for optimized geometric and energetic parameters are shown in Table 1. For the conventional cluster model, we have found two most stable adsorption states, which are the <sup>3</sup>A<sub>2</sub> state with O<sub>2</sub> bond aligned at [001] direction and the <sup>1</sup>A<sub>1</sub> state with the bond aligned at [110] direction. The triplet state <sup>3</sup>A<sub>2</sub> [001] is 0.61 kcal mol<sup>-1</sup> more stable, having an optimum O–O bond length of 1.27 Å. The <sup>1</sup>A<sub>1</sub> [110] state, however, has an O–O bond which is severely lengthened from the gas phase value (1.207 Å<sup>27)</sup>) to 1.48 Å. The net charges on O<sub>2</sub> molecules are -0.71 and -1.28 in these two cases, and we assign the two adsorption species to superoxide and peroxide dioxygen, respectively. The spin densities on O<sub>2</sub> also support this assignment. The adsorption energies predicted by the cluster model, 0.1 kcal mol<sup>-1</sup> for <sup>3</sup>A<sub>2</sub> [001] and -0.51 kcal mol<sup>-1</sup> for <sup>1</sup>A<sub>1</sub> [110], clearly do not agree with experimental value of ca. 9.3 kcal mol<sup>-1</sup>.<sup>14)</sup> We further employed the DAM method on the above system with the same optimized geometries. Because the *E*(*n*)–*n* curve<sup>11)</sup> obtained from systems with a non-integer *n* of electrons transferred to the adcluster from the bulk metal shows no occurrence of electron transfer in our system, we only need to introduce the electrostatic image force correction into the energetics of the cluster model. In Table 1, we can see that the stabilization of the system by the electrostatic image force is essential for the adsorption binding en-

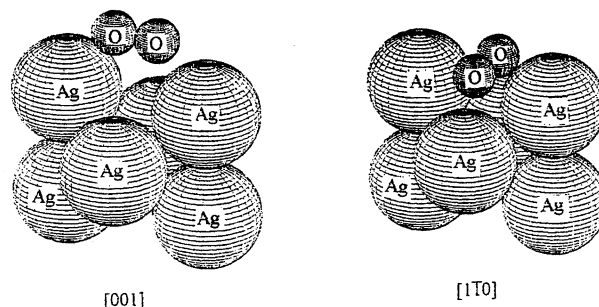


Fig. 1. Ag<sub>6</sub>–O<sub>2</sub>.

Table 1. Optimized Geometric and Energetic Parameters of Ag<sub>6</sub>–O<sub>2</sub> with Set I

Direction	State	Species	<i>R</i> <sub>O–O</sub>	<i>R</i> <sub>⊥</sub>	<i>E</i> <sub>a</sub> (CM)	<i>E</i> <sub>a</sub> (DAM) <sup>a)</sup>	Net charge	
			Å	Å	kcal mol <sup>-1</sup>	kcal mol <sup>-1</sup>	O <sub>2</sub>	O <sub>2</sub> /a. u.
[110]	<sup>1</sup> A <sub>1</sub>	O <sub>2</sub> <sup>2-</sup>	1.48	0.83	-0.51	12.50	-1.28	
	<sup>3</sup> A <sub>2</sub>	O <sub>2</sub> <sup>2-</sup>	1.49	0.82	-25.84	-12.84	-1.30	
[001]	<sup>1</sup> A <sub>1</sub>	O <sub>2</sub> <sup>2-</sup>	1.43	1.59	-36.42	-18.01	-1.26	
	<sup>3</sup> A <sub>2</sub>	O <sub>2</sub> <sup>-</sup>	1.27	1.89	0.10	6.51	-0.71	0.2106

a) *n*=0 for DAM method.

ergies, which are positive after correction and in good agreement with the experimental average value of 9.3 kcal mol<sup>-1</sup>.<sup>14)</sup> At this time, the <sup>1</sup>A<sub>1</sub> [ $\bar{1}\bar{1}0$ ] state (O<sub>2</sub><sup>2-</sup>) is obviously preferred by 6 kcal mol<sup>-1</sup> to the <sup>3</sup>A<sub>2</sub> [001] state (O<sub>2</sub><sup>-</sup>).

An orbital correlation diagram for the two most stable states, <sup>1</sup>A<sub>1</sub> [ $\bar{1}\bar{1}0$ ] and <sup>3</sup>A<sub>2</sub> [001], is given in Fig. 2. Investigating the bonding characters in detail, we see that both 4d band and 5sp band of silver give important contribution to the bonding of O<sub>2</sub> with Ag surface, as observed in earlier works.<sup>10)</sup> Simultaneously, the full-occupied  $\pi$  orbitals of O<sub>2</sub> are largely involved in the bonding process along with the  $\pi^*$  orbitals. The in-

teraction between  $\pi$  orbital of O<sub>2</sub> and 4d, 5sp band of silver is stronger in the <sup>1</sup>A<sub>1</sub> [ $\bar{1}\bar{1}0$ ] state than in the <sup>3</sup>A<sub>2</sub> [001] state. In the <sup>1</sup>A<sub>1</sub> [ $\bar{1}\bar{1}0$ ] state, the  $\pi_{\perp}$  orbital interacts with both the first and the second layer of Ag atoms, deducing a large backdonation to silver atoms. As for the <sup>3</sup>A<sub>2</sub> [001] state, the  $\pi_{\perp}$  orbital has interaction with only first layer atoms and a much smaller backdonation to silver. The  $\pi_{\parallel}^*$  orbitals of both directions accept one electron from silver to become fully occupied, but have small interactions with silver. The  $\pi_{\perp}^*$  orbital of [001] direction remains singly occupied during the adsorption process, showing a nonbonding character. The  $\pi_{\perp}^*$  orbital in the <sup>1</sup>A<sub>1</sub> [ $\bar{1}\bar{1}0$ ] state plays

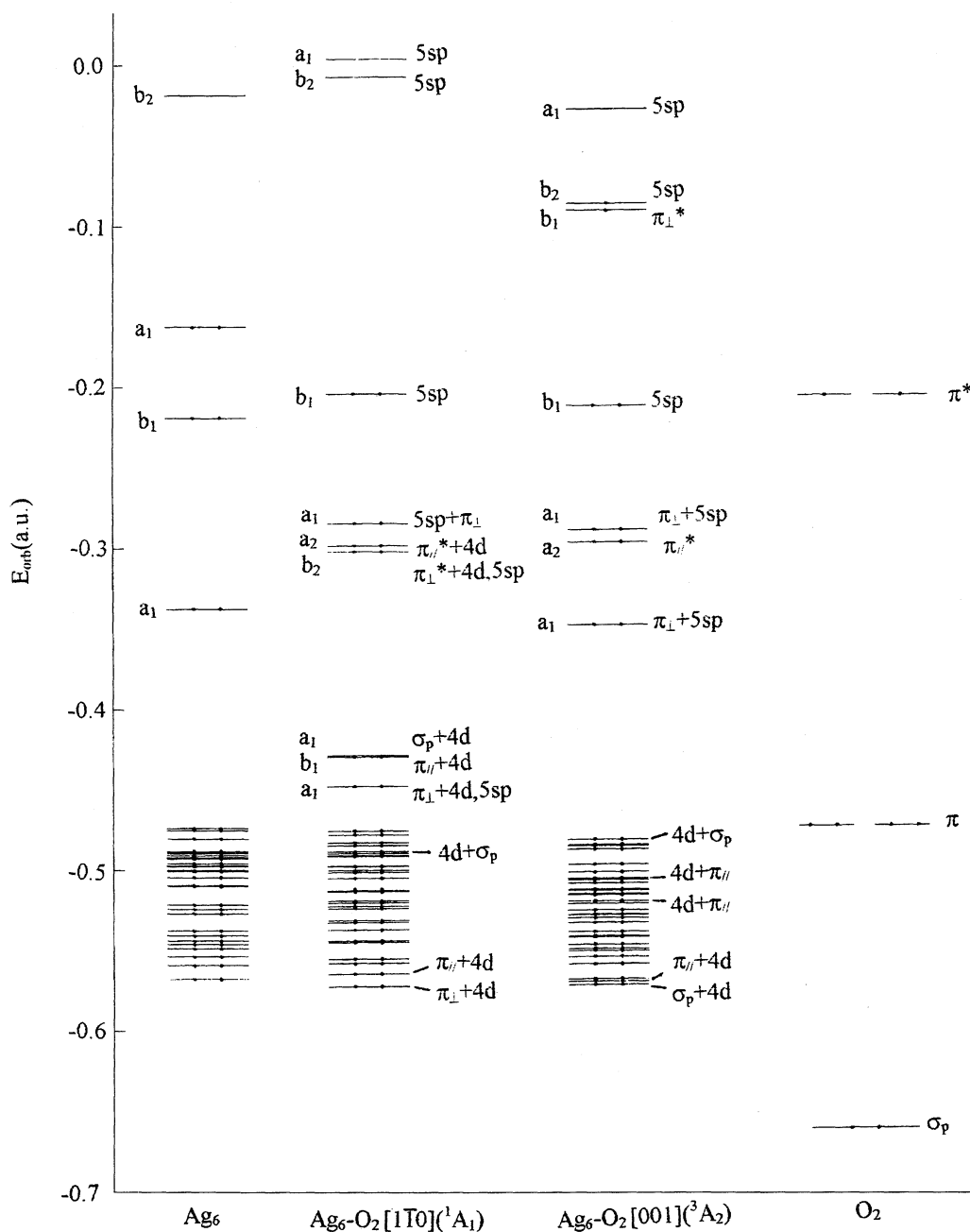


Fig. 2. Orbital correlation diagram for the two stable states.

an important role in the bonding due to its interaction with 4d and 5sp bands, resulting in a fully occupied b<sub>2</sub> orbital with bonding character. At the two adsorption geometries ([110] and [001]), the interactions of  $\pi_{\perp}$  and  $\pi_{\perp}^*$  orbitals with silver surface is the essential factor in which the different interaction leads to the different adsorption bonding of O<sub>2</sub> with the silver, namely, the O<sub>2</sub> molecule has a stronger bonding with the silver surface at the [110] direction than at the [001] azimuth.

For these two stable states, the vibrational frequencies of both the O–O stretching and Ag–O<sub>2</sub> perpendicular stretching have been calculated. The results are listed in Table 2. The directly computed values were scaled<sup>28)</sup> with reference to the calculation error of free O<sub>2</sub> molecule. The O–O frequency 732 cm<sup>-1</sup> of <sup>1</sup>A<sub>1</sub> [110] state seems to be overestimated in comparison with the experimental data in the range of 622–697 cm<sup>-1</sup>,<sup>3,4,15–18)</sup> and the frequency 1217 cm<sup>-1</sup> of <sup>3</sup>A<sub>2</sub> [001] state is closer to the result on polycrystalline reported by Rao et al.<sup>16)</sup> The calculated Ag–O<sub>2</sub> perpendicular frequencies are located in the low frequency range, which is in accordance with the observed bands. Given the errors of the experimental results themselves, the accuracy of our frequency calculations is enough to distinguish the two adsorption states. The peroxide and superoxide dioxygen species on silver surface have been widely reported experimentally,<sup>3,4,15–18,29)</sup> but on Ag (110) surface, only peroxide species has been detected.<sup>3,4)</sup> In this work, the calculated peroxide species has an O–O bond length of 1.48 Å, in excellent agreement with the NEXAFS<sup>7)</sup> result of 1.47±0.05 Å, and the vibrational frequency further confirms the assignment. The superoxide species has been identified on Ag (111),<sup>15)</sup> polycrystalline,<sup>16,17)</sup> and electrolytic silver.<sup>18)</sup> Our calculated sequence of relative thermal stability of O<sub>2</sub><sup>2-</sup> and O<sub>2</sub><sup>-</sup> coincides with the results on polycrystalline<sup>16)</sup> and electrolytic silver,<sup>18)</sup> although the <sup>3</sup>A<sub>2</sub> [001] state (O<sub>2</sub><sup>-</sup>) might not correspond exactly to one of the experimentally detected O<sub>2</sub><sup>-</sup> species. It is rational to believe that the O<sub>2</sub><sup>2-</sup> and O<sub>2</sub><sup>-</sup> species on the silver surface in different experiments may have different microscopic details, such as the adsorption site, geometry, and electronic state. For the specific long bridge site of Ag (110) surface in our study, the two possible adsorption species have widely different characteristics.

Table 2. Vibrational Frequencies of Two Stable Adsorption States

	Species	$\nu_{\text{O-O}}/\text{cm}^{-1}$	$\nu_{\perp}/\text{cm}^{-1}$
<sup>1</sup> A <sub>1</sub> [110]	O <sub>2</sub> <sup>2-</sup>	732	294
Exp.		622–697 <sup>a)</sup>	240 <sup>c)</sup>
<sup>3</sup> A <sub>2</sub> [001]	O <sub>2</sub> <sup>-</sup>	1217	249
Exp.		983–1320 <sup>b)</sup>	270 <sup>d)</sup>

a) Ref. 3, 4, 16–18, 27; b) Ref. 16–18, 27;

c) Ref. 3, 4; d) Ref. 24.

The peroxide species sits near the surface ( $R_{\perp}=0.83$  Å) in the trough of [110] direction, bonding strongly ( $E_a=12.50$  kcal mol<sup>-1</sup>) to the surface with a severely weakened O–O bond ( $\nu=732$  cm<sup>-1</sup>). It may form the precursor of dissociative adsorption through the simple dissociative mechanism along [110] grooves. The superoxide species, however, sits on the long bridge along the [001] direction away from the surface ( $R_{\perp}=1.89$  Å), weakly bonded ( $E_a=6.51$  kcal mol<sup>-1</sup>) to silver surface with a slightly weakened O–O bond ( $\nu=1217$  cm<sup>-1</sup>). Its structure and low thermal stability imply the desorption tendency of superoxide species. Recently, our in situ Raman study on electrolytic silver surface<sup>18)</sup> has given strong evidence for the similar postulation of the peroxide and superoxide species on it. For the DAM method, we have also studied the situation when one electron transfer to adcluster from bulk metal is supposed to occur. The optimized geometric and energetic parameters are shown in Table 3. Both of the adsorbed species at two directions are peroxide <sup>2</sup>B<sub>2</sub> states and have similar bond lengths, but differ in the perpendicular distances. The energetic data demonstrate that the system is more substantially stabilized than the  $n=0$  case, having much higher adsorption energies. As we have known above, the electron transfer does not occur in our system, but it will be possible if the surface potential ( $-\mu$ ) is modified by promoters or physical methods (heat, light, electric field, etc.).<sup>11)</sup> In the special case of the present work, the calculation of the  $n=1$  system implies that lowering the surface work function ( $\mu$ ) will benefit the adsorption of O<sub>2</sub> on the Ag (110) surface.

The Ag<sub>4</sub>–O<sub>2</sub> system (without the two Ag atoms of the third layer in Ag<sub>6</sub>) has also been calculated to examine the influence of cluster size. Results in Table 4 demonstrate that the adsorbed geometries do not change much, while the adsorption energies are drastically different than those on Ag<sub>6</sub> clusters. The inefficiency of Ag<sub>4</sub> cluster to reproduce adsorption energy may be mainly due to the “structure” of the cluster rather than the “size”. The Ag<sub>6</sub> cluster coincides with the “absence of dipole moment” criterion<sup>10)</sup> in choosing a cluster model, while Ag<sub>4</sub> does not. Additionally, according to Upton’s argument,<sup>10)</sup> the Ag<sub>6</sub> cluster employed here is the smallest C<sub>2v</sub> symmetric unit which is space filling if translated in the [112] and [112] direction in a three-layer slab. Therefore, the topological structure of a cluster may be more important than the size

Table 3. Optimized Geometric and Energetic Parameters of Ag<sub>6</sub>–O<sub>2</sub> with  $n=1$ <sup>a)</sup>

Direction	State	Species	$R_{\text{O-O}}$	$R_{\perp}$	$E_a$	Net charge
			Å	Å	kcal mol <sup>-1</sup>	(O <sub>2</sub> )
[110]	<sup>2</sup> B <sub>2</sub>	O <sub>2</sub> <sup>2-</sup>	1.49	0.94	25.25	-1.32
[001]	<sup>2</sup> B <sub>2</sub>	O <sub>2</sub> <sup>2-</sup>	1.45	1.64	8.84	-1.28

a) See the text for the meaning of  $n$ .

Table 4. Optimized Geometric and Energetic Parameters of Ag<sub>4</sub>-O<sub>2</sub>

Direction	Species	$R_{O-O}$	$R_{\perp}$ (Å)	$E_a$ (CM)	$E_a$ (DAM)	Net charge	Spin density
		Å	Å	kcal mol <sup>-1</sup>	kcal mol <sup>-1</sup>	O <sub>2</sub>	O <sub>2</sub> /a. u.
[110]	O <sub>2</sub> <sup>2-</sup>	1.50	0.90	-23.80	-10.37	-1.26	
	O <sub>2</sub> <sup>2-</sup>	1.50	0.80	-29.79	-17.31	-1.28	
[001]	O <sub>2</sub> <sup>2-</sup>	1.40	1.70	-40.59	-27.39	-1.04	
	O <sub>2</sub> <sup>-</sup>	1.25	1.70	-19.59	-13.35	-0.70	0.2106

Table 5. Optimized Geometric and Energetic Parameters of Ag<sub>6</sub>-O<sub>2</sub> with Set II

Direction	Species	$R_{O-O}$	$R_{\perp}$	$E_a$ (CM)	$E_a$ (DAM) <sup>a)</sup>	Net charge	Spin density
		Å	Å	kcal mol <sup>-1</sup>	kcal mol <sup>-1</sup>	O <sub>2</sub>	O <sub>2</sub> /a. u.
[110]	O <sub>2</sub> <sup>2-</sup>	1.48	0.81	-4.39	10.98	-1.42	
	O <sub>2</sub> <sup>2-</sup>	1.50	0.80	-32.62	-17.40	-1.42	
[001]	O <sub>2</sub> <sup>2-</sup>	1.43	1.58	-43.02	-21.78	-1.34	
	O <sub>2</sub> <sup>-</sup>	1.28	1.85	-0.67	7.08	-0.78	0.2146

a)  $n=0$  for DAM method.

when considering the choice of a cluster model. Lastly, a smaller basis set of Ag(3s3p4d/2s1p1d) has been applied to Ag<sub>6</sub>-O<sub>2</sub> system to investigate the basis set effect. It can be seen from Table 5 that the basis set of Ag does not affect the adsorption properties of Ag<sub>6</sub>-O<sub>2</sub> system much.

### Conclusions

Two molecular adsorption species, O<sub>2</sub><sup>2-</sup> (<sup>1</sup>A<sub>1</sub>) and O<sub>2</sub><sup>-</sup> (<sup>3</sup>A<sub>2</sub>), have been found at the long bridge site of Ag (110) surface, with the O-O bond aligned at [110] and [001] directions, respectively. Both of them are the ground states at the two adsorption geometries. The adsorption of O<sub>2</sub><sup>2-</sup> species with lengthened O-O bond of 1.48 Å and a lower vibrational frequency 732 cm<sup>-1</sup> is predicted to be more stable and leads to the dissociative adsorption, while the adsorption of O<sub>2</sub><sup>-</sup> species with an O-O bond length of 1.27 Å and frequency 1217 cm<sup>-1</sup> is predicted to be less stable and competes with desorption. The DAM method is essential to reproducing the adsorption energy. Modification in lowering the surface work function will promote the O<sub>2</sub> adsorption on silver. Cluster size and structure affect the adsorption energies substantially, but the basis set of Ag does not. However, the adsorption geometries are not perturbed by either of the two factors.

This work was supported by grants from the National Natural Science Foundation of China. We would like to thank Professor S. Iwata of Keio University in Japan for some computation time on his work station with GAMESS program.

### References

1) H. Heinemann, "Catalysis, Science and Technology," ed by R. Anderson and M. Boudart, Springer, Berlin (1981).

- 2) C. T. Campbell, *J. Vac. Sci. Technol., A*, **2**, 1024 (1984); C. T. Campbell and M. T. Paffett, *Surf. Sci.*, **139**, 396 (1984).
- 3) B. A. Sexton and R. J. Madix, *Chem. Phys. Lett.*, **76**, 194 (1980).
- 4) C. Backx, C. P. M. de Groot, and P. Biloen, *Surf. Sci.*, **104**, 309 (1981).
- 5) K. C. Prince and A. M. Bradshaw, *Surf. Sci.*, **175**, 101 (1986).
- 6) C. T. Campbell and M. T. Paffett, *Surf. Sci.*, **140**, 517 (1984).
- 7) D. A. Outka, J. Stohr, W. Jark, P. Stevens, J. Solomon, and R. J. Madix, *Phys. Rev. B*, **35**, 4119 (1987).
- 8) K. Bange, T. E. Madey, and J. K. Sass, *Chem. Phys. Lett.*, **113**, 56 (1985).
- 9) A. Selmani, J. Andzelm, and D. R. Salahub, *Int. J. Quantum Chem.*, **29**, 829 (1986).
- 10) T. H. Upton, P. Stevens, and R. J. Madix, *J. Chem. Phys.*, **88**, 3988 (1988).
- 11) H. Nakatsuji, *J. Chem. Phys.*, **87**, 4995 (1987).
- 12) H. Nakatsuji and H. Nakai, *Chem. Phys. Lett.*, **174**, 283 (1990).
- 13) H. Nakatsuji and H. Nakai, *J. Chem. Phys.*, **98**, 2423 (1993).
- 14) C. T. Campbell, *Surf. Sci.*, **157**, 43 (1985).
- 15) C. T. Campbell, *Surf. Sci.*, **173**, L641 (1986).
- 16) K. Prabhakaran and C. N. R. Rao, *Surf. Sci.*, **186**, L575 (1987).
- 17) C. Pettenkofer, I. Pockrand, and A. Otto, *Surf. Sci.*, **135**, 52 (1983).
- 18) J. Deng, X. Xu, and J. Wang, *Catal. Lett.*, **32**, 159 (1995).
- 19) K. Broomfield and R. M. Lambert, *Mol. Phys.*, **66**, 421 (1989).
- 20) H. Nakatsuji and H. Nakai, *Can. J. Chem.*, **70**, 404 (1992).
- 21) P. J. Hay and W. R. Wadt, *J. Chem. Phys.*, **82**, 270 (1985).
- 22) T. H. Dunning, Jr., and P. J. Hay, "Modern Theoretical Chemistry," ed by H. F. Schaefer, III, Plenum Press,

New York (1977), Vol. 3.

23) M. W. Schimidt, K. K. Baldrige, J. A. Boatz, J. H. Jesen, S. Koseki, M. S. Gordon, K. A. Nguyen, T. L. Windus, and S. T. Elbert, "New Version of GAMESS," *QCPE Bull.*, **10**, 52 (1990).

24) "Gaussian 92/DFT, Revision F. 2," ed by M. J. Frisch, G. W. Trucks, H. B. Schlegel, P. M. W. Gill, B. G. Johnson, M. W. Wong, J. B. Foreman, M. A. Robb, M. Head-Gordon, E. S. Replogle, R. Gomperts, J. L. Andrews, K. Raghavachari, J. S. Binkly, C. Gonzalez, R. L. Martin, D. J. Defrees, J. Baker, J. J. P. Stewart, and J. A. Pople,

Gaussian, Inc., Pittsburgh, PA (1993).

25) H. Nakatsuji, H. Nakai, and Y. Fukunishi, *J. Chem. Phys.*, **95**, 640 (1991).

26) H. Nakatsuji, *Int. J. Quantum Chem.: Quantum Chem. Symp.*, **26**, 725 (1992).

27) P. H. Krupenie, *J. Phys. Chem. Ref. Data*, **1**, 423 (1972).

28) P. Pulay, G. Fogarasi, G. Pongor, J. E. Boggs, and A. Vargha, *J. Am. Chem. Soc.*, **105**, 7037 (1983).

29) X. Wang, W. T. Tysoe, R. G. Greenler, and K. Truszkowska, *Surf. Sci.*, **258**, 335 (1991).

---